



HAL
open science

Do Current and Magnetic Helicities Have the Same Sign?

A. J B Russell, P. Démoulin, G. Hornig, D. I Pontin, S. Candelaresi

► **To cite this version:**

A. J B Russell, P. Démoulin, G. Hornig, D. I Pontin, S. Candelaresi. Do Current and Magnetic Helicities Have the Same Sign?. *The Astrophysical Journal*, 2019, 884 (1), pp.55. 10.3847/1538-4357/ab40b4 . hal-02505099

HAL Id: hal-02505099

<https://hal.sorbonne-universite.fr/hal-02505099>

Submitted on 11 Mar 2020

HAL is a multi-disciplinary open access archive for the deposit and dissemination of scientific research documents, whether they are published or not. The documents may come from teaching and research institutions in France or abroad, or from public or private research centers.

L'archive ouverte pluridisciplinaire **HAL**, est destinée au dépôt et à la diffusion de documents scientifiques de niveau recherche, publiés ou non, émanant des établissements d'enseignement et de recherche français ou étrangers, des laboratoires publics ou privés.



Do Current and Magnetic Helicities Have the Same Sign?

A. J. B. Russell¹, P. Demoulin², G. Hornig¹, D. I. Pontin¹, and S. Candelaresi¹¹ Mathematics, School of Science & Engineering, University of Dundee, Nethergate, Dundee DD1 4HN, UK; a.u.russell@dundee.ac.uk, g.hornig@dundee.ac.uk, d.i.pontin@dundee.ac.uk, s.candelaresi@dundee.ac.uk² LESIA, Observatoire de Paris, Université PSL, CNRS, Sorbonne Université, Univ. Paris Diderot, Sorbonne Paris Cité, 5 Place Jules Janssen, F-92195 Meudon, France; pascal.demoulin@obspm.fr

Received 2018 September 6; revised 2019 August 29; accepted 2019 August 29; published 2019 October 11

Abstract

Current helicity, H_c , and magnetic helicity, H_m , are two main quantities used to characterize magnetic fields. For example, such quantities have been widely used to characterize solar active regions and their ejecta (magnetic clouds). It is commonly assumed that H_c and H_m have the same sign, but this has not been rigorously addressed beyond the simple case of linear force-free fields. We aim to answer whether $H_m H_c \geq 0$ in general, and whether it is true over some useful set of magnetic fields. This question is addressed analytically and with numerical examples. The main focus is on cylindrically symmetric straight flux tubes, referred to as flux ropes (FRs), using the relative magnetic helicity with respect to a straight (untwisted) reference field. Counterexamples with $H_m H_c < 0$ have been found for cylindrically symmetric FRs with finite plasma pressure, and for force-free cylindrically symmetric FRs in which the poloidal field component changes direction. Our main result is a proof that $H_m H_c \geq 0$ is true for force-free cylindrically symmetric FRs where the toroidal field and poloidal field components are each of a single sign, and the poloidal component does not exceed the toroidal component. We conclude that the conjecture that current and magnetic helicities have the same sign is not true in general, but it is true for a set of FRs of importance to coronal and heliospheric physics.

Key words: magnetic fields – Sun: corona – Sun: heliosphere

1. Introduction

A helicity integral measures the linking of the flux of a divergence-free field, as was originally proven in the classical paper by Moffatt (1969) in the context of a vorticity field, and later made more precise by Arnold (2014). This important topological result equally applies to a magnetic field, or to the current density when the displacement current is negligible. Hence, two useful helicities—magnetic helicity and current helicity—are available in the study of magnetic fields. This paper explores one of the most fundamental questions about the relationship between those helicities: for a given magnetic field, do the current and magnetic helicities have the same sign?

Magnetic helicity is a physical invariant under conditions that are typical of many astrophysical plasmas, which raises helicity to the same special status as energy and momentum. Furthermore, helicity provides a mathematical toolset for interpreting the handedness of magnetic fields, which, in less mathematical form, has a history dating back at least a century, since it can be found in work by this journal’s founder, George Ellery Hale, and colleagues at the Mount Wilson Solar Observatory (e.g., Hale 1908; Hale et al. 1919). With these strengths, helicity has become widely applied to topics as diverse as magnetohydrodynamic (MHD) turbulence, magnetic dynamos, magnetic reconnection, turbulent relaxation (e.g., Taylor relaxation), accretion disk jets, coronal mass ejections (CMEs), coronal heating, solar filaments, active-region sigmoids, accumulation of magnetic shear at polarity inversion lines (PILs), the solar wind, and planetary magnetospheres, which are well represented in the article collections of Brown et al. (1999) and Buechner & Pevtsov (2003).

This article focuses on the sign of helicity, which is widely used in its own right. For example, the relative handedness of a pair of magnetic flux tubes is a major factor in whether and how they reconnect (Parker 1983; Linton et al. 2001; Wright 2019), which is one possibility for powering a solar flare or eruption. Hence, our title question has direct bearing on approaches to space weather forecasting that aim to assess when conditions favor magnetic reconnection. In another flagship application, the dominant signs of helicity at different latitudes and at different length scales provide important tests of solar dynamo models. The latitudinal tests encompass Hale’s polarity law for active-region magnetograms, Joy’s law for the tilt of sunspot pairs, and the hemispheric helicity rule that operates on the “chirality” of features from the scale of the quiet Sun, through active regions and filaments, to magnetic clouds in interplanetary space (see the review by Pevtsov et al. 2014, and references therein). Tests across different length scales (e.g., Singh et al. 2018) are motivated by the idea that cross-scale transport of helicity allows a dynamo to efficiently produce helicity at one scale by offsetting this with oppositely signed helicity at another scale, which is a feature of α -driven dynamos (Seehafer et al. 2003; Brandenburg & Subramanian 2005). Thus, ambiguity about the helicity’s sign would complicate efforts to reject or accept hypotheses about the origin of the Sun’s magnetic field.

1.1. Magnetic and Current Helicities

To quantify the linking of magnetic flux for a given magnetic field, \mathbf{B} , in a volume V , one first finds a vector potential \mathbf{A} such that $\mathbf{B} = \nabla \times \mathbf{A}$. Then, the basic integral for magnetic helicity is

$$H_m = \int_V \mathbf{B} \cdot \mathbf{A} \, dV.$$

A potential problem with this is that the integrand is not uniquely defined by the magnetic field (which is the field we

observe) because \mathbf{B} only defines \mathbf{A} to within addition of a gradient. This gauge issue resolves itself if \mathbf{B} is fully contained within V ($\mathbf{B} \cdot \mathbf{n} = 0$ on the boundary of V where \mathbf{n} is the surface normal) because in these cases the integral turns out to be independent of the gauge, and the integral can be precisely interpreted in terms of the Gauss linking number. However, if magnetic fields pass through the boundary of V then the above equation produces $H_m(\mathbf{B}, \mathbf{A})$, not a unique $H_m(\mathbf{B})$. A solution to this problem is to instead work with the relative magnetic helicity, which measures linking of magnetic field lines with respect to a reference field (Berger & Field 1984). The usual expression for relative helicity (Finn & Antonsen 1985) is

$$H_m = \int_V (\mathbf{B} - \mathbf{B}_{\text{ref}}) \cdot (\mathbf{A} + \mathbf{A}_{\text{ref}}) dV, \quad (1)$$

where $\mathbf{B}_{\text{ref}} = \nabla \times \mathbf{A}_{\text{ref}}$ is the reference field, with $\mathbf{B} \cdot \mathbf{n} = \mathbf{B}_{\text{ref}} \cdot \mathbf{n}$ on the boundary of V . This H_m is gauge-independent, although it does depend on the choice of reference field.

The current helicity is

$$H_c = \int_V \mathbf{J} \cdot \mathbf{B} dV, \quad (2)$$

where the current density is $\mathbf{J} = \nabla \times \mathbf{B}$, having set $\mu_0 = 1$. The value of H_c so defined is uniquely determined by \mathbf{B} , independent of the chosen gauge. We do note, though, that H_c can only be rigorously interpreted in terms of the linking of currents within V after applying considerations equivalent to those for H_m discussed above.

Comparing the two helicities, Equations (1) and (2), the advantages of the current helicity are that it is based on locally observable quantities and it is uniquely defined in all situations, unlike the relative magnetic helicity, which requires integration to find the vector potential and depends on a choice of reference field (Démoulin 2007; Pevtsov et al. 2014). Meanwhile, the magnetic helicity has the advantage of being a useful conserved quantity: magnetic helicity is exactly conserved in ideal MHD and it is approximately conserved during magnetic reconnection at high magnetic Reynolds numbers, the value of H_m varying on a significantly longer timescale than the magnetic energy (Taylor 1974; Berger 1984; Pariat et al. 2015). In broad terms then, the magnetic helicity is commonly preferred by theorists but the current helicity is more readily available to observers.

This motivates the general question: are the two helicities related in some useful way? More specifically and at the most fundamental level of comparison: do they even have the same sign? In general, or over some useful set of magnetic fields relevant to solar and interplanetary physics? This question is interesting purely as a fundamental question about magnetic structure as well.

1.2. Flux Ropes in Solar/Interplanetary Physics

The paper will make particular study of flux ropes (FRs), which are twisted magnetic flux tubes, a magnetic structure commonly encountered in many domains of plasma physics.

In the Sun, FRs are typically formed and amplified by the dynamo in the solar convective zone, in particular at its base, and when they become buoyantly unstable or are carried upward by convective motions, they may cross the photosphere to fill the corona with magnetic fields. Thus, FRs are a keystone of magnetoconvection and the build-up of active regions (e.g., Fan 2009; Hood et al. 2009a; Martínez-Sykora et al. 2015). At the photospheric level, the magnetic field is observed to be

concentrated in FRs: the largest ones form sunspots, and a full spectrum of FR sizes is observed down to the highest spatial resolutions currently observable (e.g., Borrero & Ichimoto 2011; Stenflo 2017). Coronal FRs are central to major models of flares and CMEs (e.g., Forbes 2000; Török et al. 2004; Aulanier et al. 2010). The interplanetary consequences of CMEs are observed in situ by spacecraft, as clearly identified FRs called magnetic clouds (e.g., Dasso et al. 2005; Lepping et al. 2006). Here, a full spectrum in size of FRs, with a power law, is observed (e.g., Feng et al. 2008; Janvier et al. 2014). FRs are also present in laboratory experiments, especially those designed to understand solar flares/CMEs (e.g., Tripathi & Gekelman 2013; Wongwaitayakornkul et al. 2017).

1.3. Electric Current Neutralization

Magnetic fields generally contain electric currents, and the question of whether or not solar FRs have a total electric current has been the subject of much attention and debate. As an example of this question's importance, the presence of a finite total current parallel to the FR axis is a critical issue for some CME models, because the driving force, the hoop force, depends quadratically on this total current (see Forbes 2000; Török et al. 2004; Aulanier et al. 2010). The amount of total current is also an issue for the amount of current helicity (as will be shown explicitly in Section 2.2), hence we must decide whether to make our analysis applicable to un-neutralized FRs.

If the line integral $\oint \mathbf{B} \cdot d\mathbf{r}$ around an FR is zero, then the total current is zero by Ampère's law and Stokes's theorem. However, as we will discuss in detail below, observations of the photospheric PIL in active regions frequently show a horizontal magnetic field component along the PIL, sufficient to make any line integral around one magnetic polarity non-zero, thus indicating a net current. If one trusts the measurements, then it makes sense in such cases to treat the FR as un-neutralized, presumably having become separated from neutralizing currents that remained under the photosphere. The following paragraphs provide more detail and references.

Flux ropes with the simplest twist profile have a direct current in the core, flowing parallel to the magnetic field for positively twisted FRs, surrounded by a so-called return current all around. Melrose (1995) argued from magnetic and flare observations that direct current should dominate, so that solar FRs are un-neutralized and should be rooted deep below the photosphere. This was contested by Parker (1996), who argued that FRs should be current-neutralized in the convective zone since FRs are localized by convection in small regions, and so the circulation of \mathbf{B} around an FR, and hence the total current, should vanish. In the same paper, Parker also suggested reasons why the measurements might be doubted.

Observationally, deriving the electric current from the photospheric magnetic field has several difficulties, e.g., calibration, the 180° ambiguity on the transverse magnetic field, off-disk-center problems, measurements at different height due to fibril structures, and spatial averaging of unresolved structures. Within all these limitations, recent studies from different groups continue to find that the direct current is typically greater than the surrounding return current, so in each magnetic field polarity (+/−) of an active region the electric current is un-neutralized (e.g., Wheatland 2000; Venkatakrishnan & Tiwari 2009; Georgoulis et al. 2012; Gosain et al. 2014). Also, Dalmasse et al. (2015) recently concluded that un-neutralized currents are present, using the

line-integral approach to measure net current, due to the finite magnetic shear along the PIL, and suggested that un-neutralized currents are to be generally expected in active regions and other magnetic regions.

Valuable additional insight comes from un-neutralized currents in numerical simulations with twisting motions applied to initial potential fields, and with the emergence of an FR across the photosphere (e.g., Aulanier et al. 2005; Leake et al. 2013; Török et al. 2014). In the simulations of flux emergence, the initial FR is neutralized within the convective zone, as advocated by Parker (1996), but only a fraction of the return current crosses the photosphere, making for un-neutralized current in each photospheric magnetic polarity. In other words, during flux emergence, an initial current-neutralized structure can split into two separate structures, one passing through the solar surface and the other remaining below it, neither of which is current-neutral by itself.

The conclusion of this discussion is that in this paper we will allow for the possibility of FRs carrying a net current, as well as fully current-neutral cases. Our arguments that $H_m H_c \geq 0$ under certain conditions do not assume current neutralization, and conversely our examples of $H_m H_c < 0$ do not rely on a net current.

1.4. The $H_m H_c \geq 0$ Conjecture

Although it is not often stated explicitly, there seems to be a heuristic in the community that flux tubes are either right- or left-handed, with the assumption that the magnetic and current helicities have the same sign, i.e., $H_m H_c \geq 0$. As far as we know, this was at best shown with some limited-scope examples or with a warning that this is likely not general and has not been proven rigorously (e.g., Seehafer 1990; Démoulin 2007; Pevtsov et al. 2014).

Observationally, such a principle is supported by studies showing that supposed proxies of magnetic helicity—such as the spiral pattern of chromospheric fibrils around sunspots, magnetic shear along the photospheric inversion line of active regions, magnetic tongues, and coronal sigmoids—typically provide the same sign as the current helicity (e.g., Seehafer 1990; Abramenko et al. 1996; Pevtsov et al. 1997; Burnette et al. 2004; Luoni et al. 2011; Poisson et al. 2015).

Within theory, the idea that $H_m H_c \geq 0$, at least over some useful set of magnetic fields, probably appeared empirically out of experience of model magnetic fields. The conjecture holds trivially for potential magnetic fields because $\mathbf{J} = 0 \Rightarrow H_c = 0$; there is no linking of current in the absence of current. The next type of force-free field usually encountered is a linear force-free field with $\mathbf{J} = \nabla \times \mathbf{B} = \alpha \mathbf{B}$ for constant $\alpha \neq 0$ (we have set $\mu_0 = 1$). In this case, one can choose the vector potential so that $\mathbf{B} = \nabla \times \mathbf{A} = \alpha \mathbf{A}$, which gives

$$\begin{aligned} H_m &= \int_V \mathbf{B} \cdot \mathbf{A} \, dV = \frac{1}{\alpha} \int_V B^2 \, dV, \\ H_c &= \int_V \mathbf{J} \cdot \mathbf{B} \, dV = \alpha \int_V B^2 \, dV, \\ \Rightarrow H_c &= \alpha^2 H_m. \end{aligned}$$

Thus, for linear force-free fields, $H_m H_c \geq 0$ because H_m and H_c both have the same sign as α . In this case, the result holds because the \mathbf{J} field is the same as the \mathbf{B} field scaled by the constant α ; hence, fluxes of \mathbf{J} and \mathbf{B} have the same linking. The helicity of linear force-free fields has been studied by Berger

(1985), Pevtsov et al. (1995), and Georgoulis & LaBonte (2007) among others.

The purpose of this paper is to explore the $H_m H_c \geq 0$ conjecture more generally, with a focus on FRs in MHD equilibrium.

1.5. Structure of Paper

The paper is organized as follows. Section 2 sets out our FR model with the main equations that must be solved. In Section 3, a family of FRs with direct-return current structure is explored, which highlights intuitive reasons why $H_m H_c \geq 0$ is likely to hold for many solar and heliospheric FRs. In Section 4, we present counterexamples that show $H_m H_c \geq 0$ does not hold in general, even for straight, cylindrically symmetric force-free FRs. These examples and counterexamples motivate the introduction of two further conditions, and we prove in Section 5 that force-free cylindrically symmetric FRs have the same sign of current and magnetic helicities under assumptions of no field reversals and the poloidal component not exceeding the toroidal component. The paper concludes with discussion in Section 6 and a summary of the main conclusions in Section 7.

2. Flux Rope Model

2.1. Straight Flux Rope Assumption

Writhe is known to have a significant role in determining helicity (Călugăreanu 1959; Moffatt & Ricca 1992; Berger & Prior 2006), and it is conceivable that the extra freedom afforded by writhe might produce more cases where $H_m H_c < 0$, even under conditions that are sufficient to guarantee $H_m H_c \geq 0$ in straight FRs. However, from a practical point of view, non-zero writhe complicates the modeling enough that it is worthwhile to first examine the sign of $H_m H_c$ in straight FRs without writhe. We therefore devote this paper to the simplified problem without writhe, and leave inclusion of writhe to future work.

2.2. Main Equations

To quantitatively analyze cylindrically symmetric FRs, we use cylindrical coordinates (r, ϕ, z) where the z -axis is the central axis of the FR, r is the radial coordinate, and ϕ is the azimuthal coordinate. Invariance of magnetic field components and pressure is assumed in z and ϕ . Then, $\mathbf{B} = \nabla \times \mathbf{A}$ and $\mathbf{J} = \nabla \times \mathbf{B}$ (with $\mu_0 = 1$) give

$$B_r = 0, \quad B_\phi(r) = -\frac{dA_z}{dr}, \quad B_z(r) = \frac{1}{r} \frac{d}{dr}(rA_\phi), \quad (3)$$

$$J_r = 0, \quad J_\phi(r) = -\frac{dB_z}{dr}, \quad J_z(r) = \frac{1}{r} \frac{d}{dr}(rB_\phi). \quad (4)$$

To avoid singularities at $r = 0$, we set $A_\phi(0) = 0$ and $B_\phi(0) = 0$.

The magnetic and current helicities will be evaluated for a cylindrical volume $V = [0, R] \times [0, 2\pi] \times [z_0, z_0 + 1]$, where R is the radius of the FR. The relative magnetic helicity will be measured with respect to the untwisted reference field $\mathbf{B}_{\text{ref}} = B_z(r) \mathbf{e}_z$ with $\mathbf{A}_{\text{ref}} = A_\phi(r) \mathbf{e}_\phi$, and we will use gauge freedom to set $A_z(R) = 0$ as a boundary condition. This gauge choice of $A_z(R) = 0$ is natural because it means we work in the gauge where winding with magnetic fields outside the FR is not counted. However, since we use the gauge-invariant relative

magnetic helicity, other gauge choices would lead to identical results and conclusions.

Using the above, the relative magnetic helicity, Equation (1), simplifies to

$$H_m = 4\pi \int_0^R B_\phi(r) A_\phi(r) r dr. \quad (5)$$

It is sometimes easier to work with an alternative form, which is derived by using Equation (3) to replace B_ϕ then integrating by parts, with the conditions $A_\phi(0) = 0$ and $A_z(R) = 0$, to get

$$H_m = 4\pi \int_0^R B_z(r) A_z(r) r dr. \quad (6)$$

The integrals in Equations (5) and (6) are equal despite having $B_z(r) A_z(r) \neq B_\phi(r) A_\phi(r)$ in general.

Meanwhile, the current helicity becomes

$$H_c = 2\pi \int_0^R (J_\phi B_\phi + J_z B_z) r dr. \quad (7)$$

It is possible to eliminate either J_z or J_ϕ using integration by parts, which gives the pair of alternative expressions

$$H_c = 4\pi \int_0^R J_\phi B_\phi r dr + I B_z(R), \quad (8)$$

and

$$H_c = 4\pi \int_0^R J_z B_z r dr - I B_z(R), \quad (9)$$

where

$$I = 2\pi \int_0^R J_z r dr = 2\pi R B_\phi(R) \quad (10)$$

is the total current carried by the FR. In the special case of a neutralized FR, Equations (8) and (9) are simplified by $I = 0$.

2.3. Equilibrium Condition

To ensure relevance to solar and interplanetary conditions, we restrict our search to FRs in magnetostatic equilibrium. Thus, neglecting gravity for simplicity, we require

$$\mathbf{J} \times \mathbf{B} - \nabla P = 0,$$

where P is the thermal pressure of the plasma. For a cylindrical FR, this reduces to

$$J_\phi B_z - J_z B_\phi = \frac{dP(r)}{dr}. \quad (11)$$

If we allow an unbounded thermal pressure, then the equilibrium condition is not actually a restriction because for any magnetic field we can find a balancing pressure $P(r)$ by integrating Equation (11). We are only restricted by the equilibrium condition when $P(r)$ has been prescribed or is bounded by some upper limit that is considered the maximum pressure that is physically plausible. This includes looking for force-free examples or counterexamples with $\mathbf{J} \times \mathbf{B} = \mathbf{0}$, which in cylindrical symmetry becomes

$$J_\phi B_z = J_z B_\phi. \quad (12)$$

A convenient way to build models satisfying Equation (11) is to use Equation (4) to rewrite Equation (11) as force balance

between total pressure $P_{\text{tot}} = P + B^2/2$ and magnetic tension:

$$\frac{d}{dr} \left(P + \frac{B_z^2 + B_\phi^2}{2} \right) = -\frac{B_\phi^2}{r}. \quad (13)$$

Then, if $B_\phi(r)$ and $P(r)$ are specified, and so is the value of B_z at $r = 0$, the solution for the axial field (with $B_\phi(0) = 0$ to avoid a singularity in current density on the FR axis) is

$$B_z(r) = \sqrt{B_z^2(0) + 2P(0) - 2P(r) - B_\phi^2(r) - 2 \int_0^r \frac{B_\phi^2(r')}{r'} dr'}. \quad (14)$$

3. Examples with Direct-return Current Structure

FR models in solar physics are commonly structured with a unidirectional axial magnetic field, and with a direct current in the center of the tube enclosed by a surrounding return current that completely or partially neutralizes the direct current (see Ravindra et al. 2011; Dalmasse et al. 2015, and references therein). In such a model there are intuitive reasons why $H_m H_c \geq 0$ is likely, as we explain here with the aid of some examples.

3.1. Force-free FRs with Direct-return Current Structure

For concreteness, we will illustrate the arguments using a particular set of model FRs. We look for a set of models where $B_\phi(0) = 0$ to avoid current singularity at the origin, and where $B_\phi(r)$ has a single turning point so that the FR has a direct-current region in the center surrounded by a return current. To accommodate partially neutralized as well as fully neutralized cases, we will make $B_\phi(b) = 0$ at some radius $b \geq R$, where R is the radius of the FR.

A simple function fulfilling these requirements is

$$B_\phi(r) = fr^n (b - r)^m, \quad 0 \leq r \leq R \leq b, \quad (15)$$

where $n > 0$, $m > 0$, b , and f are all constants. For all $r \in [0, R]$ (everywhere inside the FR) the poloidal field $B_\phi(r)$ has the same sign as the constant f . Using Equation (4),

$$J_z(r) = fr^{n-1} (b - r)^{m-1} ((n+1)b - (m+n+1)r), \quad (16)$$

so J_z has the same sign as the constant f for $0 \leq r < r_{\text{rev}}$, and J_z has the opposite sign to f for $r_{\text{rev}} < r$, where

$$r_{\text{rev}} = \frac{n+1}{m+n+1} b \quad (17)$$

is the radius at which J_z reverses (which may be inside or outside the FR we consider, depending on the choice of R).

To complete the model, the axial magnetic field is obtained from Equation (14), setting $P(r) = 0$ and $B_z(0) = B_0$, where the direction of the z -axis is chosen so that $B_0 > 0$. We will always choose f/B_0 small enough that B_z has a single sign within the FR, $B_z(r) > 0 \forall r \in [0, R]$, because reversals of the axial field are not commonly considered in solar FRs (e.g., Priest 2014). We also have a z -component to the vector potential, which depends on the radius R considered as the boundary of the FR:

$$A_z(r; R) = \int_r^R B_\phi(r') dr', \quad (18)$$

which comes from Equation (3) and where this integral form satisfies our chosen condition $A_z(R) = 0$. Note that within the

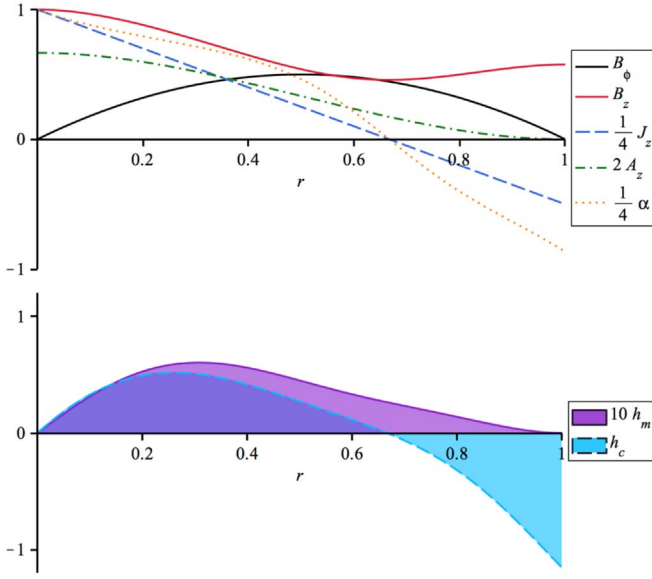


Figure 1. A current-neutralized force-free FR, with a direct current enclosed by a return current, that satisfies $H_c H_m \geq 0$. This example has $B_\phi = 2r(1-r)$, which gives $H_m = 0.4058$ and $H_c = 0.6841$ to four significant figures. Plotted quantities are scaled for easy comparison of spatial structure. Top: magnetic field components B_ϕ (black solid) and B_z (red solid), axial current J_z (blue dashed), axial component of the vector potential A_z (green dashed-dotted), and force-free parameter $\alpha = J_z/B_z$ (gold dotted). Bottom: helicity integrands $h_m = 4\pi B_z A_z r$ (light purple fill with solid edge) and $h_c = 4\pi J_z B_z r$ (light blue fill with dashed edge).

FR (for $r \in [0, R]$), A_z has the same sign as f . Finally, the magnetic and current helicities are evaluated from Equations (6) and (9).

3.2. Detailed Fully Neutralized Example

Figure 1 shows the model for $n = 1$, $m = 1$, and $f/B_0 = 2$. For calculation of A_z , and hence magnetic helicity, we have set $R = b$ to consider a fully neutralized FR with total current $I = 0$. We have chosen units with $B_0 = 1$ and $b = 1$. Figure 1 (top) plots B_ϕ , B_z , J_z , A_z , and the force-free parameter α . These have been scaled so that their spatial structure is easily seen on a common set of axes. In particular, this plot shows that this example has $B_\phi \geq 0$ with a direct current in the FR core ($J_z > 0$) and a return current at the periphery ($J_z < 0$).

This example has $H_m = 0.4058$ and $H_c = 0.6841$ to four significant figures (4 sig. fig.), so it satisfies $H_m H_c \geq 0$. Since $I = 0$ in this example, there is no boundary contribution to H_c , and so one can draw conclusions about H_m and H_c by inspecting the helicity integrands $h_m(r) = 4\pi B_z(r)A_z(r)r$ and $h_c = 4\pi J_z(r)B_z(r)r$ (see Equations (6) and (9)). Figure 1 (bottom) shows h_m and h_c as a function of the radius r within the FR. We have scaled h_m by a factor of 10 so that its spatial structure can be easily seen. While the values of H_m and H_c are similar (with the selected normalization of B_0 and $R = b$ to unity), they are reached in very different ways. In this model FR, h_m typically has a much smaller magnitude than h_c , but h_m has a single sign everywhere whereas h_c has two signs with the positive part slightly dominating the integral (Figure 1 bottom). As such, the question naturally arises: can H_m and H_c have different signs if the balance of contributions in h_c is different?

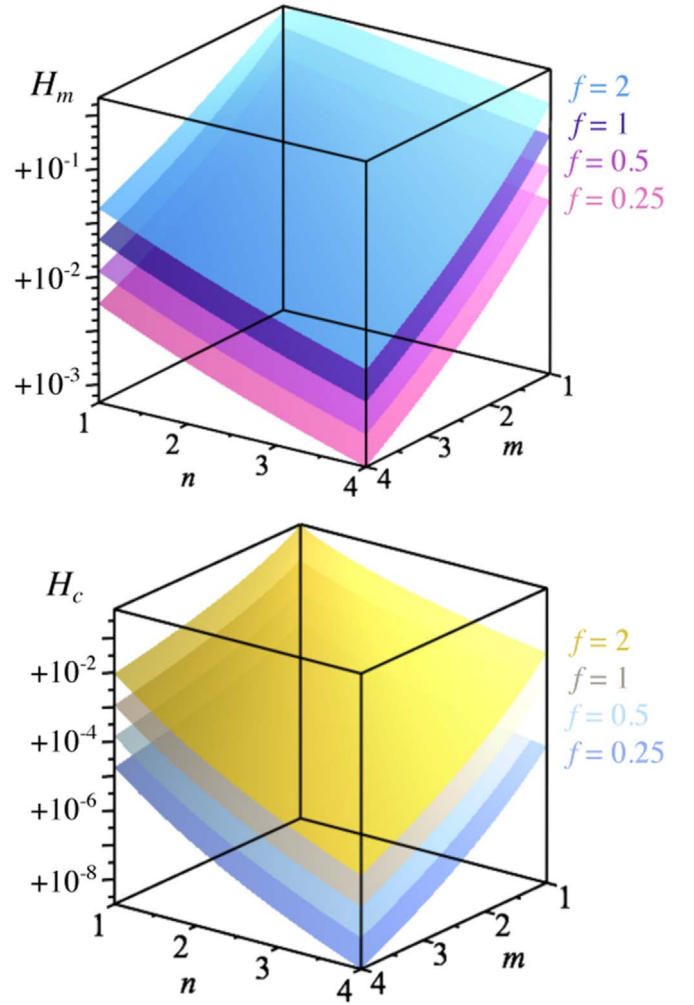


Figure 2. Magnetic helicity (top) and current helicity (bottom) for a range of fully neutralized FRs with direct-return current structure produced by $B_\phi = fr^n(1-r)^m$ (Figure 1 shows a special case with $f = 2$, $n = m = 1$). Helicity values are shown as surfaces parameterized by m and n , for four values of f : 0.25, 0.5, 1, and 2. The helicity values increase with increasing f , and decrease with increasing m and n exponents (note that the vertical axes are logarithmic). Both helicities have the same sign as B_ϕ .

3.3. Further Fully Neutralized Examples

We surveyed an extensive set of fully neutralized models with various values for f , n , and m . Figure 2 shows H_m and H_c for the parameter space $f \in \{0.25, 0.5, 1, 2\}$, $n \in [1, 4]$, $m \in [1, 4]$. As expected, H_m and H_c both increase with f (more twisted FRs). H_m and H_c also decrease for larger m and n exponents, since $B_\phi(r)$ is more concentrated in a layer located between the center and border of the FR. In every case we have checked, H_m and H_c have the same sign. This further motivates the idea that FR magnetic and current helicities may have the same sign under some widely applicable set of conditions; this will be proven rigorously in Section 5, but first, some more examples help to increase insight into reasons and necessary conditions.

3.4. Detailed Partially Neutralized Example

To explore the impact of partial neutralization, we recalculate the helicities for the example of Section 3.2 with the FR boundary at different values of $R \leq b = 1$. Changing R leaves B_z , B_ϕ , and J_z as in Figure 1 but subtracts a constant

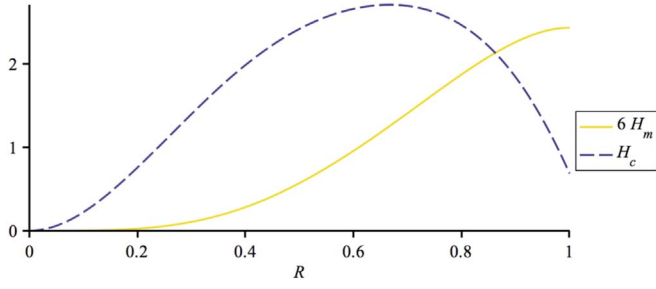


Figure 3. Magnetic and current helicities, H_m and H_c , as functions of the FR radius R . As for the example of Figure 1, $B_\phi = 2r(1 - r)$. The FR has non-zero total current when $R < 1$ and it is fully neutralized when $R = 1$. Both helicities are positive over the whole range of R .

from the original $A_z(r)$ to satisfy $A_z(R) = 0$ (see Equation (18)) and introduces a finite total current I (Equation (10)). Following these changes through, $H_m(R)$ and $H_c(R)$ depend on R as shown in Figure 3. We have scaled H_m so that it can be easily seen on the same axes as H_c . Both helicities are positive over the whole range of R , giving $H_c H_m \geq 0 \forall R \in [0, b]$.

3.5. Why $H_m H_c \geq 0$ in These Models

In the models of Sections 3.2–3.4, $B_z > 0$ and A_z has the same sign as f (since there is no reversal of $B_\phi(r)$, see Equation (18)). Therefore, referring to Equation (6), $H_m f > 0$.

Looking at the current helicity, one can use Equation (10) to write Equation (9) as

$$H_c = 2\pi \int_0^R r J_z(r) (2B_z(r) - B_z(R)) dr, \quad (19)$$

which can be viewed as an integral of rJ_z weighted by $w(r) = 2B_z(r) - B_z(R)$. Under uniform B_z , i.e., $B_z(r) = \text{constant}$ (this does not apply to the force-free model but it is helpful in laying out the argument), Equation (19) would reduce to $H_c = IB_z$, where I is zero for a neutralized FR and it has the same sign as f if the current is only partially neutralized, giving $H_c f \geq 0$ and $H_m H_c \geq 0$. If we now allow B_z to vary, in the cases we have considered B_z is on average stronger in the direct-current region than in the return-current region, which weights the integral for H_c further in favor of $H_m H_c > 0$. This is not yet a rigorous proof—that will be provided later—but it provides useful insight into why the $H_m H_c \geq 0$ conjecture frequently holds in interplanetary/solar FRs, where the axial field is typically expected to be strongest in the FR core (e.g., Lepping et al. 2006; Borrero & Ichimoto 2011).

A corollary to the above is that if the FR is only partially neutralized, as in Section 3.4, then the return current makes less of a contribution to the H_c integral, so in these cases the direct current has an even better chance of dominating to give $H_m H_c \geq 0$.

4. Counterexamples in Straight FRs

4.1. Magnetostatic Counterexample with Finite Pressure

Analysis of the examples in Section 3 showed that having larger B_z in the direct-current region than in the return-current region is an important reason for nonlinear force-free FRs having $H_m H_c \geq 0$. This immediately suggests that $H_m H_c \geq 0$ can be violated by having a high enough pressure in the core of

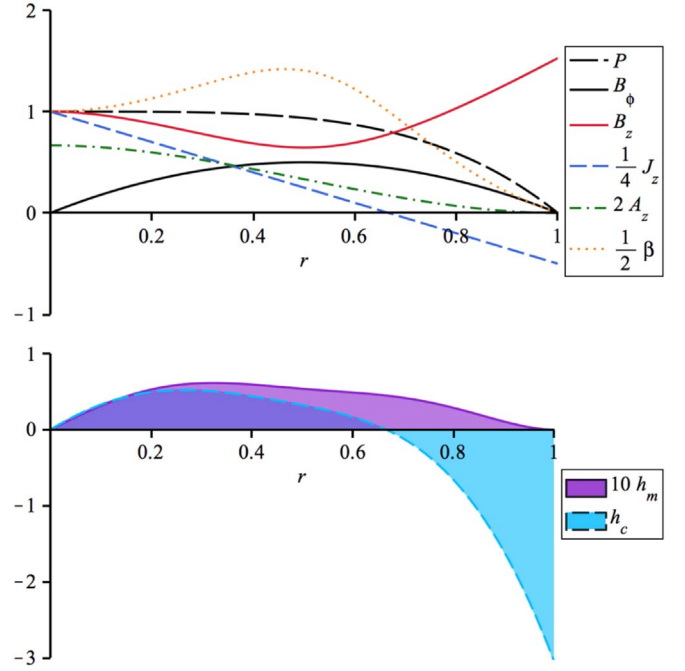


Figure 4. Counterexample to $H_m H_c \geq 0$ with high pressure in the FR core. The same model and parameters are used as for Figure 1, except a thermal plasma pressure is added following Equation (20) with a high thermal pressure in the FR core. This configuration has $H_m = 0.4917$ and $H_c = -1.838$ to 4 sig. fig., so $H_m H_c < 0$.

the FR, which according to Equation (14) reduces B_z in the high-pressure region (assuming that B_ϕ is prescribed).

To confirm this, we took the same $B_\phi(r)$ and $B_z(0)$ as in Section 3.2 but this time modified the FR by introducing

$$\frac{P(r)}{B_0^2} = 1 - \left(\frac{r}{b}\right)^4, \quad 0 \leq r \leq R \leq b, \quad (20)$$

and solving for the new $B_z(r)$ from Equation (14) in the fully neutralized case $R = b = 1$. Figure 4 plots the key quantities in the new FR, this time also showing P and the plasma beta, $\beta = P/P_m$, where $P_m = B^2/2$ is the magnetic pressure (recall that $\mu_0 = 1$). For this FR, $H_m = 0.4917$ and $H_c = -1.838$ to 4 sig. fig., so we have found a straight-axis counterexample to $H_m H_c \geq 0$. Thus we conclude that $H_m H_c \geq 0$ is not true for all magnetostatic equilibria, even if we restrict ourselves to cylindrical FRs with zero writhe and fully neutralized electric current.

4.2. Force-free Counterexample

A natural next question is whether it is possible to have $H_m H_c < 0$ for a cylindrically symmetric FR that is force-free. The answer is yes, as demonstrated by the field with

$$B_\phi(r) = \frac{1}{2} \sin(\pi r(3r - 2)), \quad 0 \leq r \leq R = 1, \quad (21)$$

and $B_z(r)$ given by Equation (14) with $P(r) = 0 \forall r$. The magnetic field components and other quantities are plotted in Figure 5. The sign of $B_\phi(r)$ is selected to have $H_m > 0$, and since $B_\phi(R) = 0$, the electric currents are fully neutralized.

This field has two signs of B_ϕ , which produces $J_z < 0$ at the core of the FR and separately in a sheath near the outer boundary, while $J_z > 0$ in a layer between those regions. In

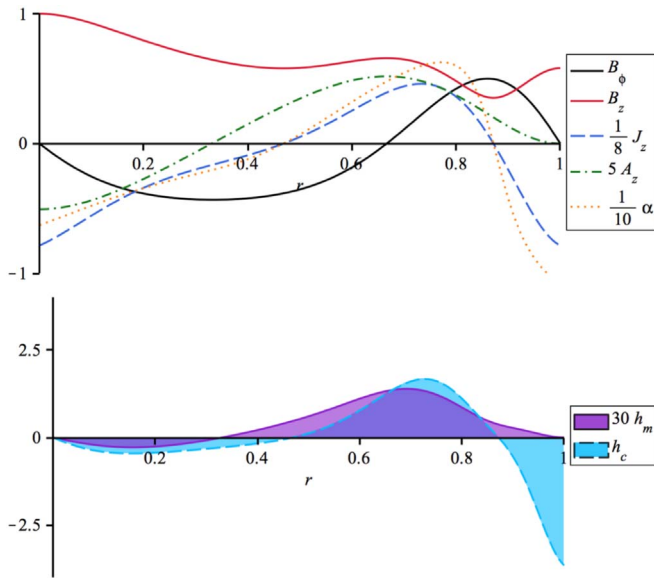


Figure 5. Force-free counterexample to $H_m H_c \geq 0$, with $B_\phi(r)$ defined by Equation (21). The major difference to the case shown in Figure 1 is that $B_\phi(r)$ changes sign and J_z has two reversals. The sign of $B_\phi(r)$ is chosen to have $H_m > 0$ for the full FR (the FR core has negative magnetic helicity). $H_m = 0.1604$ and $H_c = -0.06262$ to 4 sig. fig., so $H_m H_c < 0$.

particular, the contribution $J_z < 0$ is significant in the FR core where B_z is the largest. This provides a large negative contribution to H_c on top of the one present at the FR periphery. A_z is also negative in the FR core, but with a smaller magnitude and in a less extended region than J_z . This is also the only region to make a negative contribution to the magnetic helicity. The calculation of the helicities, Equations (6) and (9), is a consequence of the above integrand behaviors (taking into account the product with rB_z) since this case is fully neutralized ($I = 0$). Calculation gives $H_m = 0.1604$ and $H_c = -0.06262$ to 4 sig. fig. We therefore have a nonlinear force-free counterexample to the conjecture $H_m H_c \geq 0$ (which is not in conflict with the earlier results limited to linear force-free fields, discussed in Section 1.4). More counterexamples can be constructed by keeping the property of multiple reversals for J_z , allowing one to choose the sign of J_z in the FR core where the axial field is the strongest.

4.3. Applicability to Solar Environments

The counterexample of Section 4.1 has $\beta \sim 1$, which is to say the thermal pressure in the FR is comparable to the magnetic pressure, and it is in principle relevant to solar environments including the photosphere and convection zone. However, while it has a direct-return current structure, which is generally assumed to be common, B_z is stronger at the boundary of this FR ($r = 1$) than it is at the center ($r = 0$). A sunspot, for example, with such a structure would be considered highly unusual. Indeed, sunspots have lower plasma pressure and a higher magnetic field than their surroundings. Next, this counterexample does not apply to the solar corona, which has a low plasma β , i.e., the thermal pressure is much less than the magnetic pressure. Similarly, while the solar wind at 1 au typically has a plasma β of order unity, magnetic clouds have lower plasma β at their center than in the environment (e.g., Lepping et al. 2006; Rodriguez et al. 2016), which is not the case for the counterexample. We conclude that the

counterexamples due to a high plasma pressure in the core are not relevant for FRs from the photosphere, to the corona, to solar ejecta.

The counterexample of Section 4.2 is force-free and in principle relevant to solar environments including the corona and heliosphere. In particular, the axial field B_z is strongest in the center of the flux tube. However, this FR has reversal of B_ϕ , which creates a more complicated nested current structure than is assumed in most solar FR models, such as those considered in Section 3. Nonetheless, B_ϕ reversals have been seen in some solar modeling, e.g., the simulation of helicity condensation of Knizhnik et al. (2015).

The sense that the counterexamples are each in some way unusual for the photosphere, corona, or heliosphere, combined with the extensive set of examples found in Section 3, motivates the question of whether $H_m H_c \geq 0$ in a broad class of scenarios relevant in solar and interplanetary contexts.

5. Proof of $H_m H_c \geq 0$ for Force-free FRs without Field Reversals or Very Large Twist

This section presents our main result: a proof that force-free cylindrically symmetric FRs have the same sign of current and magnetic helicities under the assumptions that there are no field reversals inside the FR (B_z and B_ϕ each have a single sign for $r \leq R$) and that the poloidal component does not exceed the toroidal component ($|B_\phi/B_z| \leq 1$).

We start the proof by finding the sign of the relative magnetic helicity, which is evaluated from Equation (6). Since B_z has a single sign inside the FR, we can make $B_z > 0$ simply by orienting the coordinate system this way. Referring back to Section 3.1, A_z is determined by Equation (18) with $A_z(R) = 0$. If $B_\phi \geq 0 \forall r \in [0, R]$, then A_z is decreasing in the domain and must be positive for $r < R$, thus $H_m > 0$ since it is the integral of a positive quantity. If $B_\phi \leq 0 \forall r \in [0, R]$, then A_z is increasing on the domain and must be negative, thus $H_m < 0$ since it is the integral of a negative quantity. The sign of the magnetic helicity is therefore the same as the sign of B_ϕ .

We now turn to the current helicity. Referring to Equation (8), using Equation (4) to substitute for J_ϕ , and using Equation (10) to substitute for I ,

$$H_c = -4\pi \int_0^R B_\phi r \frac{dB_z}{dr} dr + 2\pi R B_\phi(R) B_z(R). \quad (22)$$

The integral in Equation (22) is of the form

$$f_n = \frac{4\pi(-1)^{n+1}}{(2n+1)} \int_0^R \left(\frac{B_\phi}{B_z}\right)^{2n} B_\phi r \frac{dB_z}{dr} dr \quad (23)$$

with $n = 0$. The key to our proof is that the sequence of f_n has a recursion property

$$f_n = f_{n+1} + g_n + h_n, \quad (24)$$

where

$$g_n = \frac{4\pi(-1)^n(2n+2)}{(2n+1)(2n+3)} \int_0^R B_\phi^2 \left(\frac{B_\phi}{B_z}\right)^{2n+1} dr, \quad (25)$$

$$h_n = \frac{4\pi(-1)^n}{(2n+1)(2n+3)} R B_\phi^2(R) \left(\frac{B_\phi(R)}{B_z(r)}\right)^{2n+1}. \quad (26)$$

This is proved in the [Appendix](#). Repeated application of Equation (24) to (22), from $n = 0$ to $n = N - 1$, generates

$$\begin{aligned} H_c &= f_0 + 2\pi RB_\phi(R)B_z(R) \\ &= f_1 + g_0 + h_0 + 2\pi RB_\phi(R)B_z(R) = \dots \\ &= f_N + \sum_{n=0}^{N-1} g_n + \sum_{n=0}^{N-1} h_n + 2\pi RB_\phi(R)B_z(R). \end{aligned} \quad (27)$$

Furthermore

$$f_N \rightarrow 0 \quad \text{when } N \rightarrow \infty \quad \text{if} \quad \left| \frac{B_\phi}{B_z} \right| \leq 1 \quad \forall r \in [0, R] \quad (28)$$

(the condition is sufficient but not necessary). Hence, in the limit $N \rightarrow \infty$, Equation (27) becomes

$$H_c = \sum_{n=0}^{\infty} g_n + \sum_{n=0}^{\infty} h_n + 2\pi RB_\phi(R)B_z(R). \quad (29)$$

The proof is completed by determining the sign of H_c from the terms in Equation (29).

We obtain the sign of the sum over g_n by inspecting sums of pairs of terms, $g_n + g_{n+1}$ where n is even and the g_n are given by Equation (25) (since the series starts at $n = 0$, this does not leave any terms left over). The two terms in each pair have opposite signs. Comparing the magnitudes,

$$\left| \frac{g_{n+1}}{g_n} \right| = \frac{(2n+4)(2n+1) \left| \int_0^R B_\phi^2 (B_\phi/B_z)^{2n+3} dr \right|}{(2n+5)(2n+2) \left| \int_0^R B_\phi^2 (B_\phi/B_z)^{2n+1} dr \right|}. \quad (30)$$

Furthermore, if B_ϕ and B_z each have a single sign and $|B_\phi/B_z| \leq 1 \quad \forall r \in [0, R]$, then

$$\left| \int_0^R B_\phi^2 \left(\frac{B_\phi}{B_z} \right)^{2n+3} dr \right| \leq \left| \int_0^R B_\phi^2 \left(\frac{B_\phi}{B_z} \right)^{2n+1} dr \right|, \quad (31)$$

where we have used

$$0 \leq v(x) \leq 1 \quad \forall x \quad \Rightarrow \quad \int_a^b u(x)^2 v(x) dx \leq \int_a^b u^2(x) dx,$$

so

$$\left| \frac{g_{n+1}}{g_n} \right| < 1 \quad \forall n \geq 0. \quad (32)$$

It follows that the sign of the terms with even n determines the sign of the sum over g_n . If $B_\phi \geq 0 \quad \forall r \in [0, R]$, then the even terms are positive, which gives this sum the same sign as H_m . If $B_\phi \leq 0 \quad \forall r \in [0, R]$, then the even terms are negative, which again gives this sum the same sign as H_m .

In fully neutralized cases, $B_\phi(R) = 0$ hence terms in Equation (29) apart from the sum over g_n are exactly zero. We have therefore proven that $H_m H_c \geq 0$ if the FR is fully neutralized in addition to the assumptions stated at the start of this section.

To finish, we examine the effect of the terms in Equation (29) involving $B_\phi(R) \neq 0$ when the FR is partially neutralized. Since we have oriented our coordinates so that $B_z > 0$, it follows that the term $2\pi RB_\phi(R)B_z(R)$ has the same sign as $B_\phi(R)$, and it therefore has the same sign as H_m . The sign of the sum over h_n is obtained by the same approach as used for the sign of the sum over g_n . Inspecting Equation (26),

h_n has the same sign as $B_\phi(R)$ when n is even, and the opposite sign when n is odd. Comparing the magnitudes of successive terms, h_n and h_{n+1} ,

$$\left| \frac{h_{n+1}}{h_n} \right| = \frac{(2n+1) \left(\frac{B_\phi(R)}{B_z(R)} \right)^2}{(2n+5)}, \quad (33)$$

and using $|B_\phi/B_z| \leq 1 \quad \forall r \in [0, R]$, we get

$$\left| \frac{h_{n+1}}{h_n} \right| < 1 \quad \forall n \geq 0. \quad (34)$$

Thus, if we group the series into pairs $h_n + h_{n+1}$ with n even (so as to cover the whole series), the two terms have opposite signs, but the even term has greater magnitude and therefore every pair has the same sign as B_ϕ . By extension, the full sum over h_n has the same sign as $B_\phi(R)$, which is the same as the sign of H_m . We have just shown that when the second and third terms on the right-hand side of Equation (29) are non-zero, they have the same sign as H_m . Thus, the proof holds for partially neutralized FRs as well as fully neutralized ones.

We have now proven that $H_m H_c \geq 0$ for a force-free cylindrically symmetric FR under the assumptions of no reversals in B_z or B_ϕ , and $|B_\phi| \leq |B_z|$.

6. Discussion

How realistic are the assumptions used in the proof of Section 5 for solar and interplanetary physics, what purpose did they serve, and what would happen if they were relaxed?

Starting with the assumption that $|B_\phi/B_z| \leq 1$, this holds widely in solar and interplanetary physics. An important reason is that solar FRs are typically much longer than their diameter, and so a solar FR that did not have $|B_\phi/B_z| \leq 1$ would be kink-unstable (Hood et al. 2009b). This condition is still typically valid in magnetic clouds even if much flux is added around the initial unstable FR during the eruption (e.g., Qiu et al. 2007). In the proof of Section 5, $|B_\phi/B_z| \leq 1$ was used to obtain the series form of H_c and to compare the magnitudes of consecutive terms in the series. It is therefore a convenient assumption for the proof, but more generally it is not a necessary condition because, referring back to the example models of Section 3.1, a fully neutralized case with $f = 2.2$, $n = 1$, and $m = 1$ has $|B_\phi/B_z| > 1$ over a significant subinterval of $[0, R]$, but this FR nonetheless has $H_m = 0.3582$ and $H_c = 1.065$ to four significant figures, which gives $H_m H_c \geq 0$.

Now what about the assumption that neither B_z nor B_ϕ has reversals? Photospheric magnetograms frequently show mixing of magnetic polarities, so one should be cautious about modeling an entire active region as a single FR with axial field in one direction. Nonetheless, such bipolar models are sometimes used as convenient approximations of active regions when focusing on the larger scales (e.g., Yeates et al. 2007; Zuccarello et al. 2015). At finer scales, observations of coronal loops and prominences motivate modeling substructures as FRs with axial field in one direction. A reversal of the axial field is also typically not present within magnetic clouds, or at least occurs only near their boundary (e.g., Lepping & Wu 2010). Thus, various applications in solar and interplanetary environments correspond to $B_z(r)$ having one sign in a straightened FR model. This is different to laboratory plasmas, where reversals of axial field are not unusual and may be spontaneously generated, e.g., the reversed field pinch (Taylor 1974).

Reversals of B_ϕ were excluded from the proof primarily because of the counterexample of Section 4.2 and because, with a few exceptions, most of the FR models used by solar and interplanetary physicists do not have reversals of B_ϕ . Note that even with this restriction on B_ϕ , there is considerable freedom in the pattern of axial current, J_z , which can have multiple layers of opposite sign separated by turning points of B_ϕ . Our proof therefore applies more generally than the examples and arguments of Section 3, which were based on a simple direct-return current pattern.

In the proof of Section 5, the assumed absence of magnetic field reversals conveniently allowed us to compare consecutive terms in the sum of integrals (see Equation (31)). It is not, however, a necessary assumption for $H_m H_c \geq 0$: exploring the family of force-free FRs with

$$B_\phi = \frac{\sin(\pi r(3r - 2))}{2 + ar^2}, \quad 0 \leq r \leq R = 1, \quad (35)$$

more generally than the counterexample of Section 4.2 (which had $a = 0$), we find that the fully neutralized force-free case with $a = 20$ has $H_m = -0.005186$ and $H_c = -0.04584$ (4 sig. fig.), giving $H_m H_c \geq 0$, despite the field having a reversal of B_ϕ .

While the proof assumed that the FR is exactly force-free with $\mathbf{J} \times \mathbf{B} = 0$, the conclusions are relevant to coronal and heliospheric FRs. In the corona, force-free magnetic fields are generally regarded as a good approximation, so it seems that neither a finite thermal pressure with $\beta \ll 1$ nor gravity would be likely to change the sign of $H_m H_c$. In the heliosphere, although the ambient β is of order unity, superposed epoch analysis shows that β is typically around 0.2 at the center of magnetic clouds (e.g., Rodriguez et al. 2016), so force-free fields are a reasonable first approximation here as well. Furthermore, in the heliospheric case β is larger at the periphery of the FR than in its center, and β is even greater in the external environment outside the FR. Thus, applying the reasoning of Section 4.1 to a heliospheric FR with a direct-return current structure, the effect of the thermal pressure is to further increase B_z in the direct-current region compared to B_z in the return-current region, reinforcing $H_m H_c \geq 0$.

Finally, how important is the assumption of a straight, cylindrically symmetric FR likely to be? Starting with our model's circular cross section, observed FRs can be asymmetric about the central axis. For magnetic clouds, this is especially true of the fast ones (e.g., Masías-Meza et al. 2016). It is plausible that transforming a symmetric flux tube into an asymmetric one by ideal motions will preserve the sign of $H_m H_c$ in many or perhaps even all cases, but we have not explored that question here. We have also not yet determined whether writhe provides sufficient freedom to obtain $H_m H_c < 0$ in nonlinear force-free FRs without magnetic field reversals. We therefore speculate that the result $H_m H_c \geq 0$ should hold more widely than for the cylindrically symmetric FRs covered by the proof in Section 5, but we advocate caution until these issues can be clarified by future investigations.

7. Conclusions

This paper has examined whether or not magnetic fields must have magnetic and current helicities of the same sign, i.e., is there a unique handedness for H_m and H_c ?

In general, magnetic fields can have oppositely signed H_m and H_c , making the handedness of such fields ambiguous, even

when B_ϕ has a single sign. We found concrete examples of $H_m H_c < 0$ by considering a magnetostatic FR with high pressure at its center (Section 4.1), and a nonlinear force-free FR with reversals of B_ϕ (Section 4.2).

Our main conclusion, though, is that $H_m H_c \geq 0$ for a set of FRs relevant to the photosphere, corona, and interplanetary space. This is supported most rigorously by the mathematical proof in Section 5 that cylindrically symmetric force-free FRs have $H_m H_c \geq 0$, assuming $|B_\phi/B_z| < 1$ and no field reversals (the assumptions are sufficient, but as shown by examples in Section 6, not necessary for $H_m H_c \geq 0$). Complementing this proof, Section 3 explored intuitive reasons why $H_m H_c \geq 0$ holds in FRs with a direct-return current structure: the direct current contributes to H_c with the same sign as H_m , whereas the return current contributes with the opposite sign, and in realistic photospheric/coronal/interplanetary conditions, stronger B_z in the direct-current region weights the sum in favor of $H_m H_c \geq 0$. Similarly, if the return current does not fully cancel the direct current, then the return current makes less of a contribution to H_c , which also favors $H_m H_c \geq 0$. These arguments give confidence that $H_m H_c \geq 0$ should not rely on the circular cross section or the force-free condition $\mathbf{J} \times \mathbf{B} = 0$ assumed in the proof of Section 5, provided these more general considerations are satisfied.

Finally, various avenues remain open for future work. Perhaps the most notable of these is to establish whether or not writhe can produce $H_m H_c < 0$ for typical coronal/interplanetary conditions—the next step to justify continued use of the $H_m H_c \geq 0$ heuristic in these fields—and to extend our analysis to FRs with non-circular cross section. We therefore hope to see further work on the question “When do current and magnetic helicities have the same sign?” in future years.

We thank the anonymous reviewer for helpful comments that improved the manuscript. The University of Dundee Solar MHD Group gratefully acknowledge support from STFC under consortium grants ST/K000993/1 and ST/N000714/1. This paper was prompted by discussions during a research visit of P.D. to the University of Dundee, which was kindly funded by the Northern Research Partnership (which is supported by The Scottish Funding Council) and organized by Dr. Miho Janvier. This research has made use of NASA's Astrophysics Data System Bibliographic Services.

Appendix Proof of the Recursion Formula

Since we consider force-free fields, Equation (4) and (12) combine to give

$$r \frac{dB_z}{dr} = -\frac{B_\phi}{B_z} \frac{d}{dr}(rB_\phi). \quad (36)$$

Using this to replace $r dB_z/dr$ in Equation (23), then integrating by parts with $B_\phi(0) = 0$,

$$f_n = K_1 + \frac{4\pi(-1)^{n+1}}{(2n+1)} \int_0^R r B_\phi \frac{d}{dr} \left(\frac{B_\phi^{2n+2}}{B_z^{2n+1}} \right) dr, \quad (37)$$

where

$$K_1 = \frac{4\pi(-1)^n R B_\phi^{2n+3}(R)}{(2n+1) B_z^{2n+1}(R)}. \quad (38)$$

Next, we use the product rule and chain rule to separate the integral as

$$\begin{aligned}
 f_n &= K_1 + \frac{4\pi(-1)^{n+1}}{(2n+1)} \int_0^R r B_\phi^{2n+3} \frac{d}{dr} \left(\frac{1}{B_z^{2n+1}} \right) dr \\
 &\quad + \frac{4\pi(-1)^{n+1}(2n+2)}{(2n+1)} \int_0^R \frac{r B_\phi^{2n+2}}{B_z^{2n+1}} \frac{dB_\phi}{dr} dr \\
 &= K_1 + \frac{4\pi(-1)^{n+1}}{(2n+1)} \int_0^R r B_\phi^{2n+3} \frac{d}{dr} \left(\frac{1}{B_z^{2n+1}} \right) dr \\
 &\quad + \frac{4\pi(-1)^{n+1}(2n+2)}{(2n+1)(2n+3)} \int_0^R \frac{r}{B_z^{2n+1}} \frac{d}{dr} (B_\phi^{2n+3}) dr,
 \end{aligned} \tag{39}$$

which after another integration by parts becomes

$$\begin{aligned}
 f_n &= K_1 + K_2 + \frac{4\pi(-1)^{n+1}}{(2n+1)} \int_0^R r B_\phi^{2n+3} \frac{d}{dr} \left(\frac{1}{B_z^{2n+1}} \right) dr \\
 &\quad + \frac{4\pi(-1)^n(2n+2)}{(2n+1)(2n+3)} \int_0^R B_\phi^{2n+3} \frac{d}{dr} \left(\frac{r}{B_z^{2n+1}} \right) dr,
 \end{aligned} \tag{40}$$

where

$$K_2 = \frac{4\pi(-1)^{n+1}(2n+2)}{(2n+1)(2n+3)} \frac{R B_\phi^{2n+3}(R)}{B_z^{2n+1}(R)}. \tag{41}$$

Using the product rule in the last integral,

$$\begin{aligned}
 f_n &= K_1 + K_2 + \frac{4\pi(-1)^{n+1}}{(2n+1)} \int_0^R r B_\phi^{2n+3} \frac{d}{dr} \left(\frac{1}{B_z^{2n+1}} \right) dr \\
 &\quad + \frac{4\pi(-1)^n(2n+2)}{(2n+1)(2n+3)} \int_0^R \frac{B_\phi^{2n+3}}{B_z^{2n+1}} dr \\
 &\quad + \frac{4\pi(-1)^n(2n+2)}{(2n+1)(2n+3)} \int_0^R r B_\phi^{2n+3} \frac{d}{dr} \left(\frac{1}{B_z^{2n+1}} \right) dr,
 \end{aligned} \tag{42}$$

and collecting terms algebraically gives

$$\begin{aligned}
 f_n &= \frac{4\pi(-1)^{n+1}}{(2n+1)(2n+3)} \\
 &\quad \times \int_0^R r B_\phi^{2n+3} \frac{d}{dr} \left(\frac{1}{B_z^{2n+1}} \right) dr + g_n + h_n
 \end{aligned} \tag{43}$$

where g_n is defined in Equation (25) and $h_n = K_1 + K_2$ produces Equation (26). Finally, differentiating in the first integral yields

$$f_n = \frac{4\pi(-1)^{n+2}}{(2n+3)} \int_0^R r \frac{B_\phi^{2n+3}}{B_z^{2n+2}} \frac{dB_z}{dr} dr + g_n + h_n \tag{44}$$

and working through to the finish gives

$$\begin{aligned}
 f_n &= \frac{4\pi(-1)^{(n+1)+1}}{2(n+1)+1} \\
 &\quad \times \int_0^R \left(\frac{B_\phi}{B_z} \right)^{2(n+1)} B_\phi r \frac{dB_z}{dr} dr + g_n + h_n \\
 &= f_{n+1} + g_n + h_n,
 \end{aligned} \tag{45}$$

as required.

ORCID iDs

A. J. B. Russell  <https://orcid.org/0000-0001-5690-2351>
P. Demoulin  <https://orcid.org/0000-0001-8215-6532>
G. Hornig  <https://orcid.org/0000-0003-0981-2761>
D. I. Pontin  <https://orcid.org/0000-0002-1089-9270>
S. Candelaresi  <https://orcid.org/0000-0002-7666-8504>

References

- Abramenko, V. I., Wang, T., & Yurchishin, V. B. 1996, *SoPh*, **168**, 75
Arnold, V. I. 2014, in *Collected Works, Volume II: Hydrodynamics, Bifurcation Theory, and Algebraic Geometry*, ed. A. B. Givental et al. (Berlin: Springer), 357
Aulanier, G., Démoulin, P., & Grappin, R. 2005, *A&A*, **430**, 1067
Aulanier, G., Török, T., Démoulin, P., & DeLuca, E. E. 2010, *ApJ*, **708**, 314
Berger, M. A. 1984, *GApFD*, **30**, 79
Berger, M. A. 1985, *ApJS*, **59**, 433
Berger, M. A., & Field, G. B. 1984, *JFM*, **147**, 133
Berger, M. A., & Prior, C. 2006, *JPhA*, **39**, 8321
Borrero, J. M., & Ichimoto, K. 2011, *LRSP*, **8**, 4
Brandenburg, A., & Subramanian, K. 2005, *PhR*, **417**, 1
Brown, M. R., Canfield, R. C., & Pevtsov, A. A. (ed.) 1999, *Magnetic Helicity in Space and Laboratory Plasmas*, Vol. 111 (Washington, DC: AGU)
Buechner, J., & Pevtsov, A. A. (ed.) 2003, *Advances in Space Research*, Vol. 32, *Magnetic Helicity at the Sun*, in *Solar Wind and Magnetospheres* (Amsterdam: Elsevier)
Burnette, A. B., Canfield, R. C., & Pevtsov, A. A. 2004, *ApJ*, **606**, 565
Călugăreanu, G. 1959, *CzMJ*, **11**, 588
Dalmasse, K., Aulanier, G., Démoulin, P., et al. 2015, *ApJ*, **810**, 17
Dasso, S., Mandrini, C. H., Démoulin, P., Luoni, M. L., & Gulisano, A. M. 2005, *AdSpR*, **35**, 711
Démoulin, P. 2007, *AdSpR*, **39**, 1674
Fan, Y. 2009, *LRSP*, **6**, 4
Feng, H. Q., Wu, D. J., Lin, C. C., et al. 2008, *JGRA*, **113**, A12105
Finn, J. M., & Antonsen, J. T. M. 1985, *CoPPC*, **9**, 111
Forbes, T. G. 2000, *JGR*, **105**, 23153
Georgoulis, M. K., & LaBonte, B. J. 2007, *ApJ*, **671**, 1034
Georgoulis, M. K., Titov, V. S., & Mikić, Z. 2012, *ApJ*, **761**, 61
Gosain, S., Démoulin, P., & López Fuentes, M. 2014, *ApJ*, **793**, 15
Hale, G. E. 1908, *ApJ*, **28**, 100
Hale, G. E., Ellerman, F., Nicholson, S. B., & Joy, A. H. 1919, *ApJ*, **49**, 153
Hood, A. W., Archontis, V., Galsgaard, K., & Moreno-Insertis, F. 2009a, *A&A*, **503**, 999
Hood, A. W., Browning, P. K., & van der Linden, R. A. M. 2009b, *A&A*, **506**, 913
Janvier, M., Démoulin, P., & Dasso, S. 2014, *SoPh*, **289**, 2633
Knizhnik, K. J., Antiochos, S. K., & DeVore, C. R. 2015, *ApJ*, **809**, 137
Leake, J. E., Linton, M. G., & Török, T. 2013, *ApJ*, **778**, 99
Lepping, R. P., Berdichevsky, D. B., Wu, C.-C., et al. 2006, *AnGeo*, **24**, 215
Lepping, R. P., & Wu, C. C. 2010, *AnGeo*, **28**, 1539
Linton, M. G., Dahlburg, R. B., & Antiochos, S. K. 2001, *ApJ*, **553**, 905
Luoni, M. L., Démoulin, P., Mandrini, C. H., & van Driel-Gesztelyi, L. 2011, *SoPh*, **270**, 45
Martínez-Sykora, J., Moreno-Insertis, F., & Cheung, M. C. M. 2015, *ApJ*, **814**, 2
Masías-Meza, J. J., Dasso, S., Démoulin, P., Rodríguez, L., & Janvier, M. 2016, *A&A*, **592**, A118
Melrose, D. B. 1995, *ApJ*, **451**, 391
Moffatt, H. K. 1969, *JFM*, **35**, 117

- Moffatt, H. K., & Ricca, R. L. 1992, *RSPSA*, 439, 411
- Pariat, E., Valori, G., Démoulin, P., & Dalmasse, K. 2015, *A&A*, 580, A128
- Parker, E. N. 1983, *ApJ*, 264, 635
- Parker, E. N. 1996, *ApJ*, 471, 485
- Pevtsov, A. A., Berger, M. A., Nindos, A., Norton, A. A., & van Driel-Gesztelyi, L. 2014, *SSRv*, 186, 285
- Pevtsov, A. A., Canfield, R. C., & McClymont, A. N. 1997, *ApJ*, 481, 973
- Pevtsov, A. A., Canfield, R. C., & Metcalf, T. R. 1995, *ApJL*, 440, L109
- Poisson, M., López Fuentes, M., Mandrini, C. H., & Démoulin, P. 2015, *SoPh*, 290, 3279
- Priest, E. 2014, *Magnetohydrodynamics of the Sun* (Cambridge: Cambridge Univ. Press)
- Qiu, J., Hu, Q., Howard, T. A., & Yurchyshyn, V. B. 2007, *ApJ*, 659, 758
- Ravindra, B., Venkatakrishnan, P., Tiwari, S. K., & Bhattacharyya, R. 2011, *ApJ*, 740, 19
- Rodríguez, L., Masías-Meza, J. J., Dasso, S., et al. 2016, *SoPh*, 291, 2145
- Seehafer, N. 1990, *SoPh*, 125, 219
- Seehafer, N., Gellert, M., Kuzanyan, K. M., & Pipin, V. V. 2003, *AdSpR*, 32, 1819
- Singh, N. K., Käpylä, M. J., Brandenburg, A., et al. 2018, *ApJ*, 863, 182
- Stenflo, J. O. 2017, *SSRv*, 210, 5
- Taylor, J. B. 1974, *PhRvL*, 33, 1139
- Török, T., Kliem, B., & Titov, V. S. 2004, *A&A*, 413, L27
- Török, T., Leake, J. E., Titov, V. S., et al. 2014, *ApJL*, 782, L10
- Tripathi, S. K. P., & Gekelman, W. 2013, *SoPh*, 286, 479
- Venkatakrishnan, P., & Tiwari, S. K. 2009, *ApJL*, 706, L114
- Wheatland, M. S. 2000, *ApJ*, 532, 616
- Wongwaitayakomkul, P., Haw, M. A., Li, H., Li, S., & Bellan, P. M. 2017, *ApJ*, 848, 89
- Wright, A. N. 2019, *ApJ*, 878, 102
- Yeates, A. R., Mackay, D. H., & van Ballegooijen, A. A. 2007, *SoPh*, 245, 87
- Zuccarello, F. P., Aulanier, G., & Gilchrist, S. A. 2015, *ApJ*, 814, 126